1000-0569/2014/030(01)-0095-08 *Acta Petrologica Sinica* 岩石学报

内蒙古镶黄旗哈达庙地区晚古生代中酸性侵入岩的年代学、地球化学、Sr-Nd 同位素组成及其地质意义*

刘军[1] 武广[1**] 李铁刚[2] 王国瑞[1] 吴昊[2]

LIU Jun[1], WU Guang[1**], LI TieGang[2], WANG GuoRui[1] and WU Hao[2]

1. 中国地质科学院矿产资源研究所,国土资源部成矿作用与资源评价重点实验室,北京 100037
2. 中国地质大学,北京 100083
1. *MLR Key Laboratory of Metallogeny and Mineral Assessment*, *Institue of Mineral Resources*, *Chinese Academy of Geological Sciences*, *Beijing* 100037, *China*
2. *China University of Geosciences*, *Beijing* 100083, *China*

2013-08-20 收稿, 2013-11-30 改回.

Liu J, Wu G, Li TG, Wang GR and Wu H. 2014. SHRIMP zircon U-Pb dating, geochemistry, Sr-Nd isotopic analysis of the Late Paleozoic intermediate-acidic intrusive rocks in the Hadamiao area, Xianghuang Banner, Inner Mongolia and its geological significances. *Acta Petrologica Sinica*, 30(1):95-108

Abstract The Hadamiao area is located in the northern margin of the North China plate. The SHRIMP U-Pb dating of zircons from granite porphyry and diorite of the Hadamiao area yields ages of 271 ± 3Ma and 267 ± 3Ma. Granite porphyry is characterized by its high SiO_2 (averaging 75.11%) and K_2O contents (averaging 5.06%), low MgO (averaging 0.43%), Cr (averaging 6.70×10^{-6}), Ni (averaging 5.15×10^{-6}) and V contents (averaging 26.86×10^{-6}), but diorite is characterized by its lower SiO_2 (averaging 57.28%) and K_2O contents (averaging 1.23%), higher MgO (averaging 5.31%), Cr (averaging 195.18×10^{-6}), Ni (averaging 59.11×10^{-6}) and V contents (averaging 148.13×10^{-6}), respectively. The rare earth elements (REE) contents have an obvious increase from diorite to granite porphyry, but granite porphyry has more strongly negative Eu anomalies and fractional degree of heavy REE (HREE) and light REE (LREE). These rocks are enriched in large ion lithophile elements (LILE), but depleted in high field strength elements (HFSE). Both granite porphyry and diorite share the common features of relative high I_{Sr} valeus (I_{Sr}: 0.704803 ~ 0.707025), low $\varepsilon_{Nd}(t)$ values ($\varepsilon_{Nd}(t)$: -3.92 ~ 1.03) and young Nd-model age (898 ~ 1322Ma). We suggest that granite porphyry and diorite of the Hadamiao area were formed during a middle Permian subduction of paleo-Asian ocean slab. The high Mg diorite was a product of partial melting of mantle wedge replaced by slab-derived fluid and mixed by crustal materials, and granite porphyry was probable a product of crystallization differentiation of dioritic magma.

Key words Intermediate-acidic intrusive rocks; Zirocn SHRIMP U-Pb age; Geochemistry; Hadamiao; Central Asia Orogenic Belt

摘 要 内蒙古哈达庙地区位于华北板块北缘,本文对区内花岗斑岩和闪长岩进行了锆石 SHRIMP U-Pb 定年,其形成年龄分别为 271 ±3Ma 和 267 ±3Ma。花岗斑岩具有高的 SiO_2 含量(均值 75.11%)、较高的 K_2O 含量(均值 5.06%)、低的 MgO 含量(均值 0.43%)及低的 Cr(均值 6.70×10^{-6})、Ni(均值 5.15×10^{-6})和 V(均值 26.86×10^{-6})含量,闪长岩与花岗斑岩相比具有更低的 SiO_2(均值 57.28%)和 K_2O 含量(均值 1.23%),更高的 MgO(均值 5.31%)、Cr(均值 195.18×10^{-6})、Ni(均值 59.11×10^{-6})和 V(均值 148.13×10^{-6})含量。从闪长岩到花岗斑岩,稀土元素总量增加,铕负异常更明显,轻重稀土分馏程度增大。两者均富集大离子亲石元素、贫高场强元素、强烈亏损 Nb、Ta、P 和 Ti 等元素,具有较高的锶初始比值(I_{Sr}:0.704803 ~0.707025)、较低的钕初始比值($\varepsilon_{Nd}(t)$:-3.92 ~1.03)和相对年轻的 Nd 模式年龄(898 ~1322Ma)。哈达庙地区花岗斑岩

---

* 本文受国家自然科学基金项目(41172081、41202058)、"十一·五"国家科技支撑计划项目(2006BAB01A02)和中国地质调查局地质调查项目(1212011085260)联合资助.

第一作者简介: 刘军,男,1983 年生,博士,助理研究员,矿床学专业,E-mail: junliu@yeah.net

** **通讯作者**:武广,男,1965 年生,博士,研究员,矿床学和地球化学专业,E-mail: wuguang65@163.com

和闪长岩形成于中二叠世古亚洲洋的俯冲过程,高镁闪长岩是受俯冲板片流体交代的地幔楔部分熔融形成的熔体上升过程中受到地壳物质混染的产物,而花岗斑岩很可能是闪长质岩浆结晶分异的产物。

关键词 中酸性侵入岩;锆石 SHRIMP U-Pb 年龄;地球化学;哈达庙;中亚造山带

中图法分类号 P588.121; P588.122; P597.3

中亚造山带是全球显生宙陆壳增生与改造最显著的大陆造山带(Jahn *et al.*, 2000; Wu *et al.*, 2000; Badarch *et al.*, 2002; Xiao *et al.*, 2003; 何国琦和朱永峰,2006),同时也是世界上最重要的铜、金、钼、铅锌及稀有稀土金属矿产地之一(洪大卫等,2003;Chen *et al.*, 2007;杨富全等,2007;周振华等,2010; Zhou *et al.*, 2012; 刘军等,2013a,b,c;毛景文等,2013),是研究造山带大陆生长、构造演化及成矿作用过程的天然场所。目前,中亚造山带最终碰撞的时间、地点及方式等问题仍存在争议,在缝合带位置上,存在索伦山-林西地区(Wang and Liu, 1986)、二连-贺根山地区(曹从周等,1986;Şengör *et al.*, 1993)和西拉木伦-长春-延吉一线(Wu *et al.*, 2002)等观点,在缝合时间上,大多数学者认为我国北山或包头以西地区的缝合时代为石炭纪末,东部西拉木伦河一带的缝合时代为二叠纪末(毛景文等,2002a,b,2005;高俊等,2006;Li, 2006;李锦轶等,2006,2013),但也有部分学者主张缝合时间为三叠纪末(Xiao *et al.*, 2008)。区域上发育不同时代(早古生代、晚古生代、早中生代)、不同岩石类型花岗岩类(与俯冲、碰撞有关的花岗岩类,与造山后伸展有关的A型花岗岩),已经构成我国重要的成矿带(童英等,2010)。

目前,研究者更多地关注于中亚造山带内部的岩浆-热液活动及相关成矿作用(毛景文等,2002a,b,c;Yang *et al.*, 2006, 2009;Zhang *et al.*, 2008, 2010; Liu *et al.*, 2012;张作衡等,2012;刘军等,2010,2013a,b,c),但对中亚造山带与华北克拉通结合部岩浆岩的侵位时代、地球化学属性及源区性质缺乏研究。内蒙古镶黄旗哈达庙地区中酸性侵入岩位于华北板块北缘的温都尔庙俯冲-增生杂岩带内,区域内构造岩浆活动频繁,其中夹杂着众多前寒武纪地块、高压变质岩和条带状蛇绿岩带,正确认识该区域内各期岩浆-热液活动的时空关系及其成因对探讨古亚洲洋在华北克拉通北侧的俯冲过程及其闭合时限具有重要意义。本课题组对哈达庙地区进行了1:1万区域地质填图工作,掌握了本区详细的第一手基础地质资料。本文针对哈达庙地区的花岗斑岩和闪长岩开展了岩石学、岩石地球化学、同位素地球化学和SHRIMP 锆石 U-Pb 定年的工作,探讨了中酸性侵入岩的地球化学性质、成因及其形成的地球动力学背景。

1 区域地质及岩体特征

哈达庙地区位于内蒙古中部镶黄旗西北约20km处,大地构造位置位于温都尔庙俯冲-增生杂岩带内(图1)。区内出露地层较简单,主要由第四系和下二叠统包特格组构成。第四系主要为砂砾、粉砂和风成砂,分布于研究区的东部、东北部及区内的3条冲沟内。下二叠统包特格组主要为中细粒长石石英砂岩,夹少量的粉砂岩和泥岩,局部见含砾砂岩,主要分布在研究区的西南部(图2a)。区内岩浆岩分布广泛,主要有闪长岩、花岗闪长岩、二长花岗岩、花岗斑岩及少量隐爆火山角砾岩脉和流纹岩脉(图2a, b)。闪长岩在区内大面积分布,侵入下二叠统包特格组。二长花岗岩和花岗闪长岩区内少量出露,侵入闪长岩或包特格组中。花岗斑岩脉分布较广泛,呈近东西向侵位到闪长岩及包特格组内,延长3km左右,近直立状产出,宽约10~30m,最宽处可达60m。隐爆角砾岩脉分布于西北部,主要由33条规模不等的隐爆火山角砾岩脉构成。流纹岩脉多沿近东西向构造断裂分布,成群出现(聂凤军和张洪涛,1989)。本区的断裂构造主要受研究区南部的赤峰-白云鄂博断裂控制,晚期遭到中生代北东向断裂及褶皱构造活动的影响(聂凤军等,1989)。

花岗斑岩 呈斑状结构,斑晶主要为石英(7%~9%)、钾长石(3%~5%)和斜长石(<1%)。石英:他形粒状,聚合晶体出现,大小在0.5~1.0mm,有的与钾长石组成聚合斑晶。钾长石:自形、半自形乃至他形均见,见卡钠复合双晶,有的与先晶出钾长石构成聚斑晶,大小在0.4~1.0mm。斜长石:半自形,板状,有聚片双晶,见绢云母化,大小在0.4~0.6mm。基质呈细晶结构,由微细晶粒的长石、石英他形晶组成,大小在0.04~0.10mm。岩石整体有轻微绢云母化。

闪长岩 半自形粒状结构,主要由斜长石(65%~75%)、角闪石(15%~20%)、黑云母(5%~8%)及石英(<3%)组成。斜长石:半自形板状,发育聚片双晶,双晶纹较宽,为中长石。斜长石晶体破碎,并存在不同程度的绢云母化,大小在0.9~2.7mm。角闪石:半自形柱状、粒状,多色性微弱,有解理,但解理纹较细,聚片双晶发育,大小在0.6~1.9mm。黑云母:片状,多色性不明显,解理发育,干涉色因绿泥石化和绿帘石化而显异常蓝色,大小在0.3~1.5mm。石英:他形粒状,表面干净,有裂纹,大小在0.3~0.8mm。

2 样品采集和分析方法

在综合分析区域地质背景及野外地质调查基础上,对闪长岩及花岗斑岩露头进行了采样(图2a,b),采集年代学测试样品2件、岩石地球化学测试样品11件。锆石分选工作在河北省区域地质调查队完成,通过常规的重选和磁选进行初选,然后在双目镜下挑出晶形和透明度较好的锆石,将锆石置于环氧树脂中,磨制约一半大小,使锆石内部暴露,用于阴极发光及随后的 SHRIMP U-Pb 分析,锆石阴极发光在中

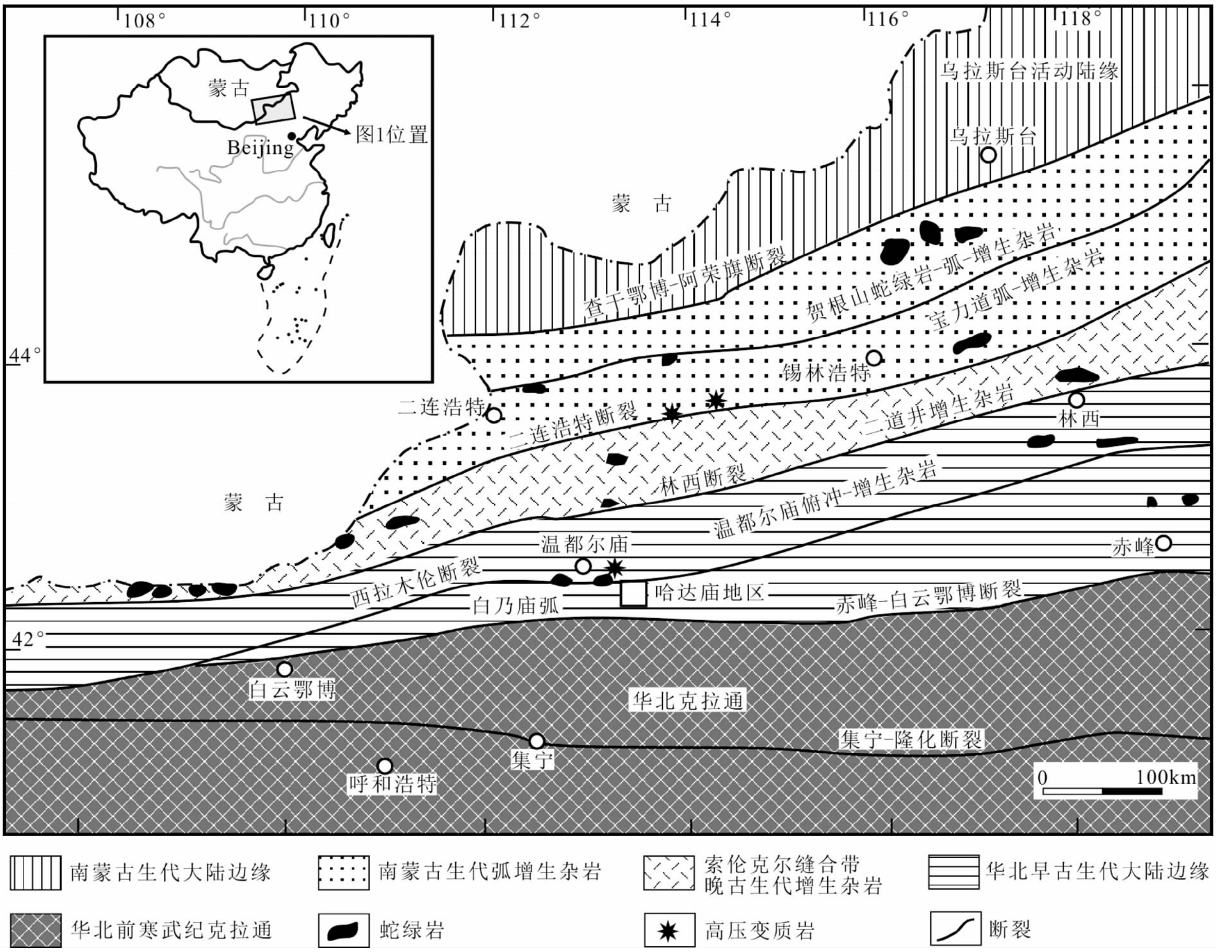

图1　内蒙古中部及其邻区区域地质图(底图据鲁颖淮等,2009)

Fig. 1　Geological map of central Inner-Mongolia and adjacent area (after Lu *et al.*, 2009)

国地质科学院矿产资源研究所电子探针研究室完成,锆石 SHRIMP U-Pb 分析在北京离子探针中心 SHRIMP Ⅱ上完成,详细分析流程和原理参考 Williams (1998)、刘敦一等(2003)和简平等(2003)的文章,一次离子流强度约 7.5nA,加速电压约 10kV,样品靶上的离子束斑直径约 25～30μm。应用澳大利亚国家地调局标准锆石 TEM(417Ma)进行元素间的分馏校正。应用 RSES(澳大利亚国立大学地学院)标准锆石 SL13(年龄 572Ma;U 含量 238×10^{-6})标定所测锆石的 U、Th 和 Pb 含量。数据处理采用国际标准程序 ISOPLOT (ver 3.0)。表 1 中所列单次测量的数据点的误差均为 1σ。采用^{206}Pb/^{238}U 年龄,其加权平均值具 95% 的置信度。

岩石主量、稀土和微量元素测试由国土资源部廊坊地球物理地球化学勘查研究所完成。其中全岩主量元素采用 XRF 分析,稀土和微量元素采用 ICP-MS 分析。主量元素分析精度优于 3%,稀土和微量元素分析精度优于 5%。Sr、Nd 同位素分析在中国科学院广州地球化学研究所超净实验室进行前处理。Sr 和 REE 分离采用 AG50-8X 离子交换柱,分别收集 Sr 和 REE 解析液;REE 的分离采用 HDEHP 交换柱,收集 Nd 解析液,测试工作在北京大学造山带实验室完成,测试所用实验仪器为 VG Axiom HR-MC-ICP-MS,Sr 和 Nd 同位素比值用^{86}Sr/^{88}Sr = 0.1194 和^{146}Nd/^{144}Nd = 0.7219 作质量分馏校正。实验室对 Sr 标样 NIST SRM 987 测定结果为^{87}Sr/^{86}Sr = 0.710255 ± 15 (2σ),对 Nd 标样 Shin-Etsu JNdi-1 测定结果为^{143}Nd/^{144}Nd = 0.512121 ± 9 (2σ)。^{87}Rb/^{86}Sr 和^{143}Nd/^{144}Nd的测试精度优于 2% 和 0.5%。

3　锆石 SHRIMP U-Pb 年龄

花岗斑岩(HK3):锆石为无色到浅褐色,玻璃光泽,透明-半透明,无包体,呈短柱状-长柱状,大小 150～300μm,长宽比 1.2∶1～3∶1。从阴极发光图像上看,所有锆石均发育韵律环带和明暗相间的条带结构,显示了岩浆成因锆石的特征(图 3a)。锆石 U-Pb 测年结果见表 1,11 个点的测试结果显示锆石的 Th/U 比值介于 0.73～1.24 之间,均大于 0.1,属于典型的岩浆成因锆石。在锆石 U-Pb 年龄谐和图中(图 4a),所有分析数据都分布在谐和线上及附近,11 个点的年龄数据在 259.1～277.8Ma 之间,^{206}Pb/^{238}U 年龄的加权平均

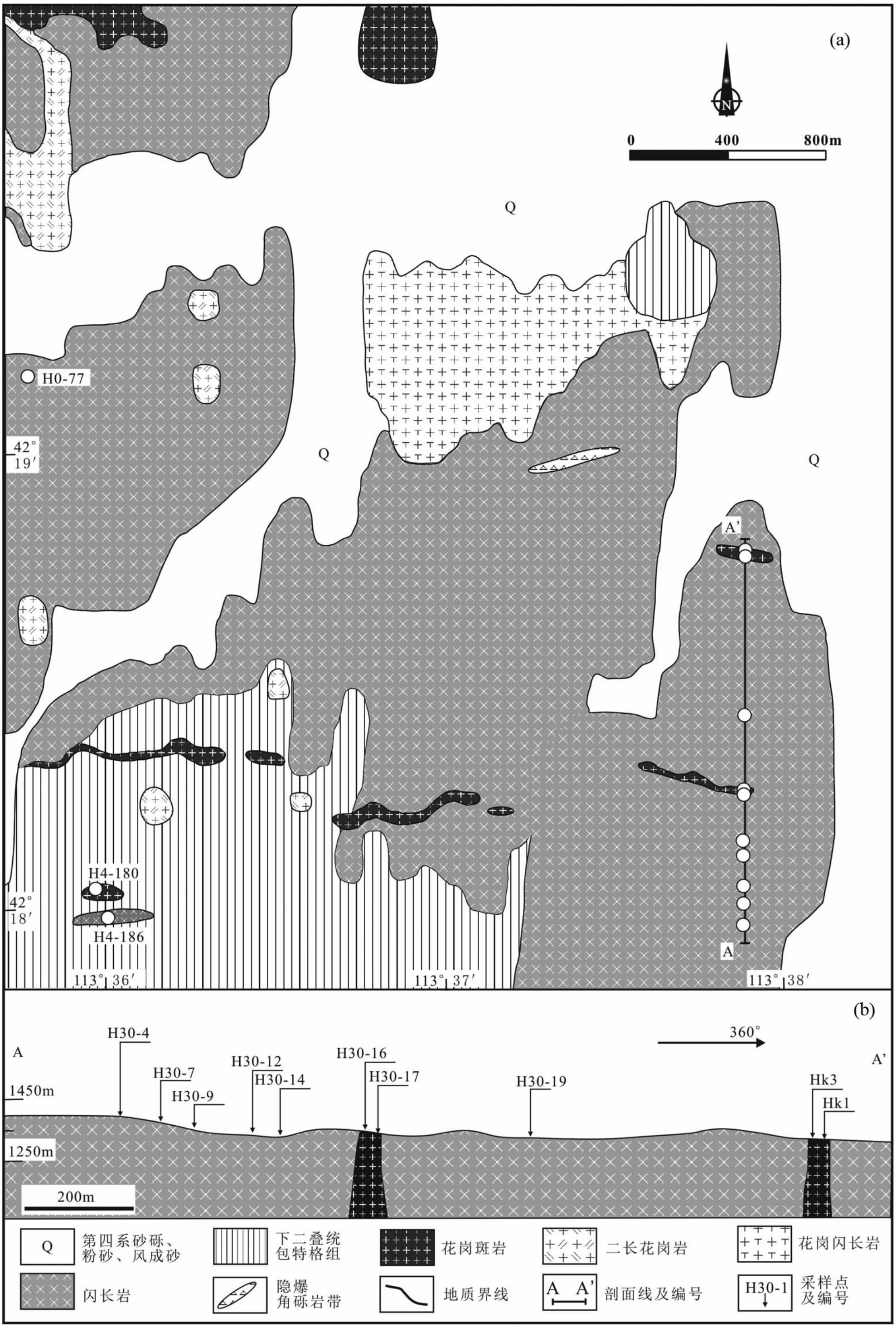

图 2 哈达庙地区地质简图(a)和采样剖面图(b)

Fig. 2 Sketch geological map (a) and sampling profile (b) of the Hadamiao area

值为 271 ± 3Ma, MSWD = 1.1。

闪长岩(H30-19):锆石呈无色到浅褐色,透明-半透明,无包体发现,为短柱状-长柱状,大小 150 ~ 300μm,长宽比 1.5 : 1 ~ 3 : 1。锆石阴极发光显示,锆石均发育明暗相间的条带结构及韵律环带结构,显示锆石为岩浆成因的锆石(图 3b)。对该样品测定了 11 个单颗粒锆石,显示锆石的 Th/U 比值介于 0.71 ~ 1.24 之间,均大于 0.1,为典型的岩浆成因锆石。从表 1 中可以看出,11 个点的年龄数据比较集中,分布在 259.6 ~ 275.4Ma 之间,$^{206}Pb/^{238}U$ 年龄的加权平均值为 267 ± 3Ma, MSWD = 1.5(图 4b)。

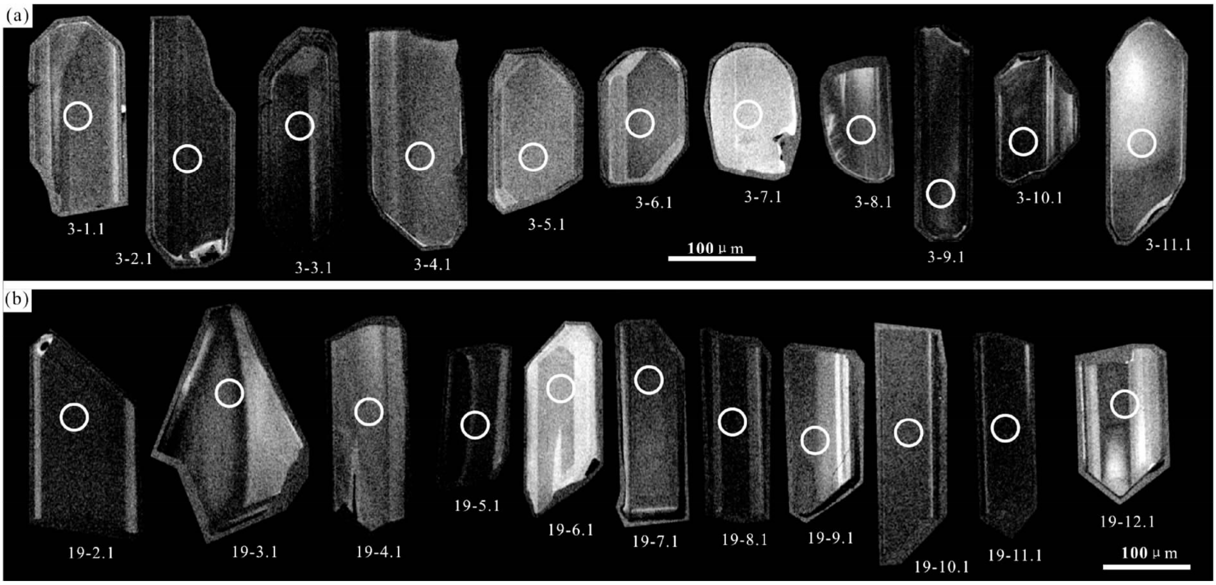

图 3　哈达庙地区花岗斑岩和闪长岩中锆石的形态及分析点位图

Fig. 3　Cathodoluminescence (CL) images of zircons from granite porphyry and diorite from the Hadamiao area

Circles in zircon crystals indicate positions of SHRIMP U-Pb analytical sites. 3-1.1: Number of analyzed spot

表 1　哈达庙地区中酸性侵入岩锆石 SHRIMP U-Pb 测试结果

Table 1　SHRIMP U-Pb isotopic analyses for zircons of intermediate-acidic intrusive rocks from the Hadamiao area

测点号	$^{206}Pb_c$ (%)	U ($\times 10^{-6}$)	Th ($\times 10^{-6}$)	$^{232}Th/^{238}U$	$^{206}Pb^*$ ($\times 10^{-6}$)	$^{206}Pb/^{238}U$ 年龄(Ma)		$^{207}Pb^*/^{206}Pb^*$	±%	$^{207}Pb^*/^{235}U$	±%	$^{206}Pb^*/^{238}U$	±%
HK3-1.1	0.28	864	923	1.10	31.9	270.9	±4.6	0.04946	2.0	0.2927	2.7	0.04291	1.7
HK3-2.1	0.11	1193	1475	1.28	44.7	274.8	±4.7	0.05020	1.2	0.3014	2.1	0.04355	1.7
HK3-3.1	0.43	634	663	1.08	23.9	275.8	±4.9	0.0495	3.5	0.298	4.0	0.04371	1.8
HK3-4.1	0.45	335	274	0.85	12.3	269.6	±4.8	0.0516	3.2	0.304	3.7	0.04271	1.8
HK3-5.1	0.33	399	361	0.93	14.8	272.1	±5.6	0.0497	4.2	0.295	4.7	0.04312	2.1
HK3-6.1	0.20	307	276	0.93	11.4	271.5	±5.2	0.0491	3.1	0.291	3.7	0.04302	2.0
HK3-7.1	0.20	258	213	0.85	9.35	265.9	±4.9	0.0501	2.8	0.2908	3.3	0.04211	1.9
HK3-8.1	0.45	383	342	0.92	14.6	277.8	±4.9	0.0506	3.7	0.307	4.1	0.04403	1.8
HK3-9.1	0.05	657	687	1.08	23.2	259.1	±4.7	0.05143	1.6	0.2908	2.4	0.04102	1.8
HK3-10.1	0.34	672	731	1.12	25.0	272.6	±4.7	0.05070	1.7	0.3020	2.5	0.04320	1.8
HK3-11.1	—	185	135	0.76	6.78	270.6	±5.0	0.0530	3.2	0.313	3.7	0.04286	1.9
H30-19-2.1	0.21	751	808	1.11	27.6	269.3	±4.6	0.0498	2.2	0.2928	2.8	0.04266	1.8
H30-19-3.1	0.00	752	752	1.03	26.6	260.0	±4.6	0.05257	1.5	0.2983	2.3	0.04116	1.8
H30-19-4.1	0.61	183	130	0.73	6.55	261.9	±5.0	0.0506	5.6	0.289	5.9	0.04147	1.9
H30-19-5.1	0.08	643	619	1.00	23.1	263.7	±4.6	0.05197	1.7	0.2992	2.5	0.04176	1.8
H30-19-6.1	0.44	221	192	0.89	8.07	267.0	±5.0	0.0500	4.8	0.291	5.1	0.04229	1.9
H30-19-7.1	0.00	742	812	1.13	26.2	259.6	±4.5	0.05092	1.4	0.2886	2.3	0.04110	1.8
H30-19-8.1	0.13	783	859	1.13	28.7	268.7	±4.6	0.05003	1.8	0.2937	2.5	0.04257	1.8
H30-19-9.1	0.41	428	402	0.97	15.7	268.0	±4.7	0.0494	2.6	0.2889	3.2	0.04245	1.8
H30-19-10.1	0.16	911	1128	1.28	33.9	273.4	±4.7	0.05070	1.6	0.3029	2.4	0.04333	1.8
H30-19-11.1	0.20	887	1078	1.26	33.3	274.9	±4.7	0.05016	1.6	0.3013	2.4	0.04357	1.7
H30-19-12.1	0.46	493	576	1.21	18.6	275.4	±4.8	0.0486	2.9	0.293	3.4	0.04365	1.8

注：误差为 1σ；Pb_c 和 Pb^* 分别为普通铅和放射成因铅；年龄和同位素比值均为测定的 ^{204}Pb 校正

花岗斑岩和闪长岩的锆石 U-Pb 年龄在误差范围内接近，花岗斑岩的年龄略大于闪长岩的年龄。我们在野外观察中发现花岗斑岩侵位于闪长岩中并沿东西向延伸，因此两类岩体是较短时间间隔内岩浆活动的产物，花岗斑岩的形成应

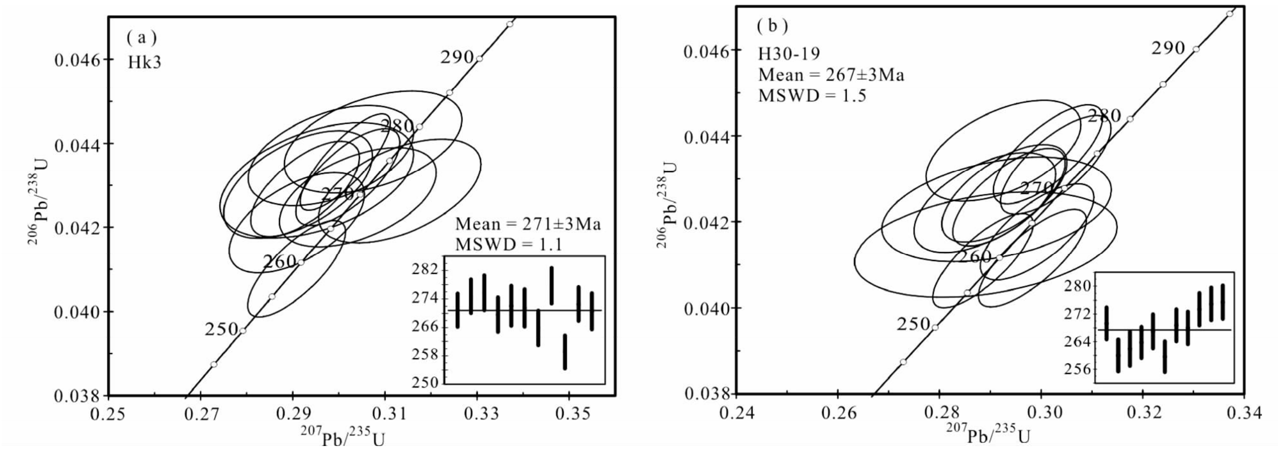

图4 哈达庙地区花岗斑岩和闪长岩锆石的 SHRIMP U-Pb 年龄谐和图

Fig. 4 Concordia diagrams of SHRIMP U-Pb zircon dating results for the granite porphyry and diorite from the Hadamiao area

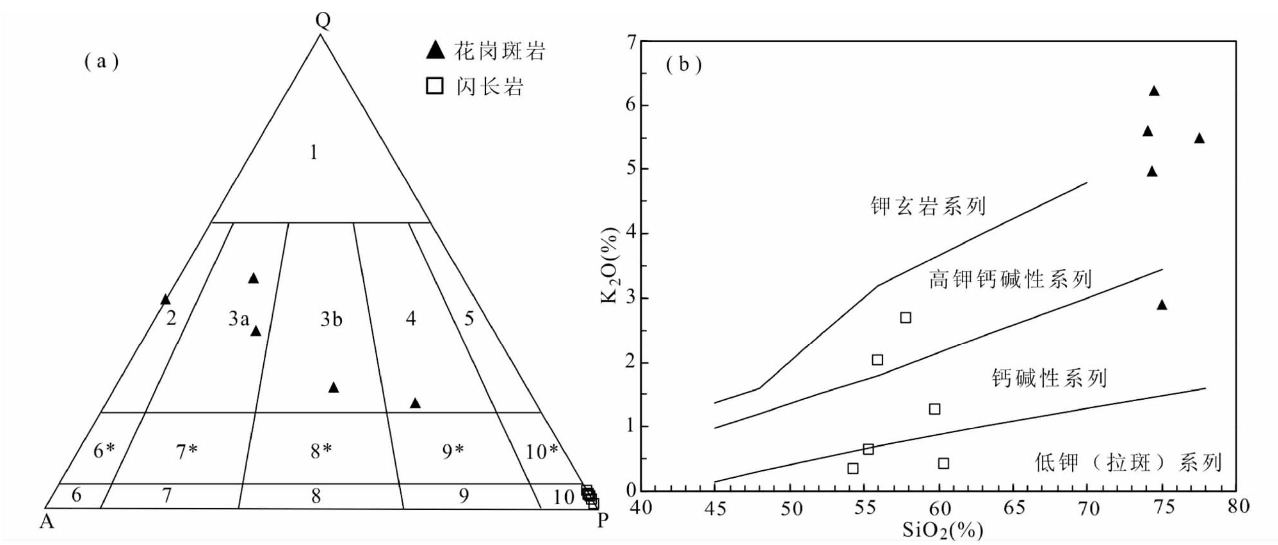

图5 哈达庙地区花岗斑岩和闪长岩的 QAP 分类图解(a, 据 Streckeisen, 1976)和 SiO_2-K_2O 关系图解(b, 据 Peccerillo and Taylor, 1976)

Fig. 5 Diagrams of QAP (a, after Streckeisen, 1976) and K_2O-SiO_2 (b, after Peccerillo and Taylor, 1976) of granite porphyry and diorite from the Hadamiao area

该略晚于闪长岩。

4 岩石地球化学

4.1 主要元素

花岗斑岩的 SiO_2 含量介于 74.13% ~77.61%，Al_2O_3 含量介于 12.40% ~14.09%，K_2O 含量介于 2.92% ~6.25%，Na_2O 含量介于 1.93% ~2.80%，K_2O/Na_2O 介于 1.27 ~3.20，MgO 含量介于 0.11% ~0.87%，$Mg^{\#}$介于 22 ~46，平均值为36，铝饱和指数介于 1.11 ~1.92(表2)。在 QAP 分类图解(图5a)中，主要落入花岗岩区域，在 SiO_2-K_2O 图解(图5b)中，投影点全部落入高钾钙碱性系列区域。花岗斑岩的 $Mg^{\#}$平均值略低于太古代 TTG(奥长花岗岩-英云闪长岩-花岗闪长岩)的平均值(平均值为 43，Drummond *et al.*, 1996; Martin *et al.*, 2005)，接近实验熔体的平均值(平均值为 40，Martin *et al.*, 2005)。TTG 所具有的低 $Mg^{\#}$是加厚的地壳底部含水的玄武质岩石部分熔融的结果(Smithies, 2000; Sheppard *et al.*, 2001; Condie, 2005)，花岗斑岩的低 $Mg^{\#}$、Ni 和 Cr 值特征，暗示其形成可能与地壳深部岩石的部分熔融有关。

闪长岩的 SiO_2 含量介于 54.43% ~60.45%，Al_2O_3 含量介于 15.61% ~17.49%，K_2O 含量介于 0.36% ~2.68%，Na_2O 含量介于 2.15% ~2.66%，K_2O/Na_2O 介于 0.17 ~1.00。闪长岩的 MgO 含量和 $Mg^{\#}$值明显高于花岗斑岩，其

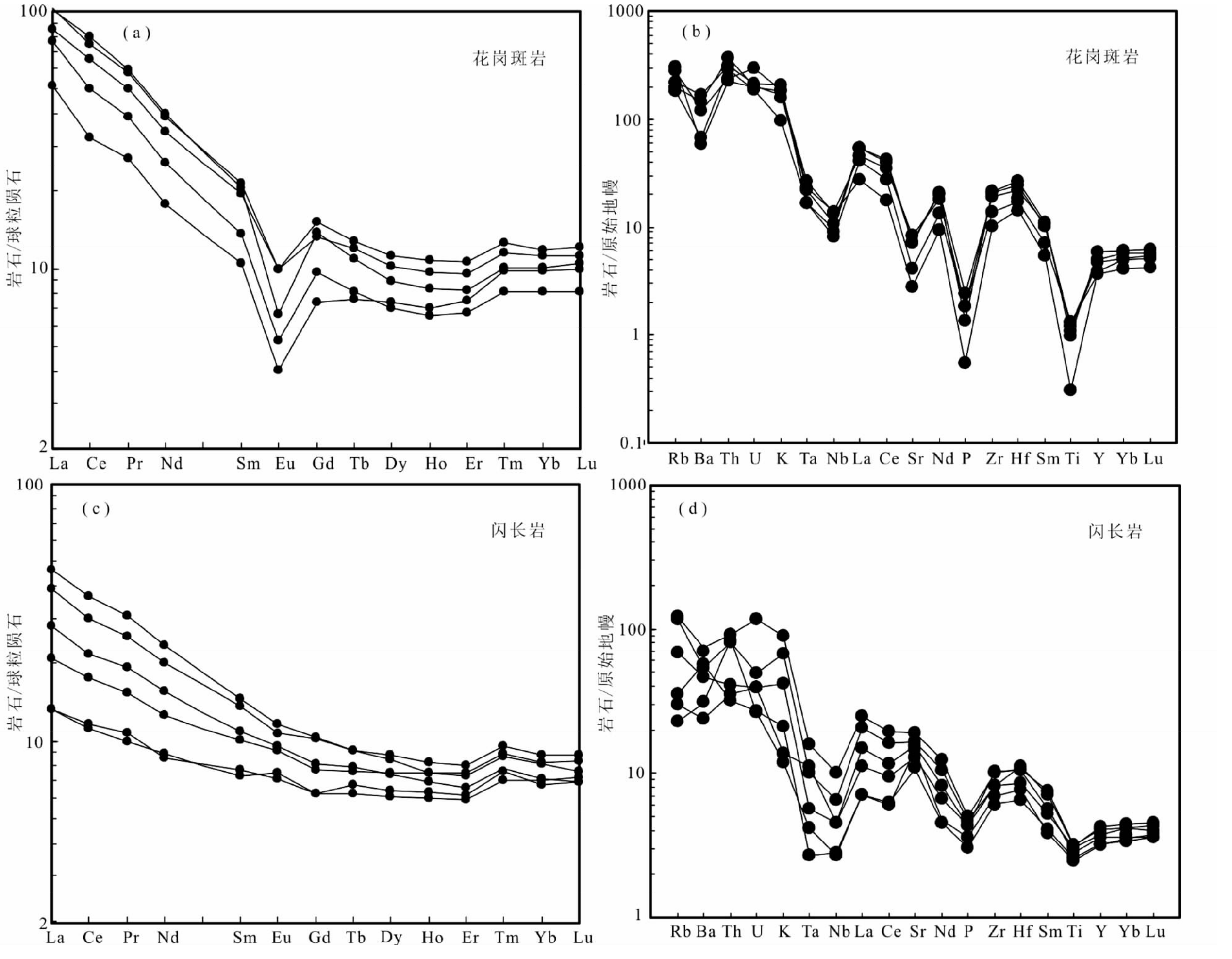

图6 哈达庙地区花岗斑岩和闪长岩稀土元素配分曲线(a、c，球粒陨石标准化值据 Boynton，1984)和微量元素原始地幔标准化蛛网图(b、d,原始地幔标准化值据 Taylor and McLennan，1985)

Fig. 6 Chondrite-normalized REE patterns (a, c, normalization values after Boynton, 1984) and primitive mantle-normalized trace elements spidergrams (b, d, normalization values after Taylor and McLennan, 1985) of granite porphyry and diorite from the Hadamiao area

MgO 含量介于3.16% ~8.56%，$Mg^{\#}$值介于48 ~69,平均值为58,铝饱和指数介于0.71 ~1.12(表2)。在 QAP 分类图解(图5a)中,投影点落入闪长岩区域,在 SiO_2-K_2O 图解(图5b)中,投影点较分散,分布于低钾系列至高钾钙碱性系列的广泛区域。

4.2 微量元素

花岗斑岩稀土元素总量介于 79.95×10^{-6} ~ 169.7×10^{-6}，$(La/Yb)_N$介于5.24 ~9.97,岩石以轻稀土元素富集和重稀土元素亏损为特征(表2和图6a)，δEu 介于0.39 ~0.60,显示铕负异常。一般认为铕负异常是斜长石分离结晶作用的表现。花岗斑岩富集 Rb、K、La、Ce 和 Nd 等大离子亲石元素及 Th、Zr 和 Hf 等高场强元素,同时强烈亏损 Ta、Nb、Sr、P 及 Ti,弱亏损 Ba(表2和图6b)。

闪长岩稀土元素总量介于 34.45×10^{-6} ~ 89.03×10^{-6}，$(La/Yb)_N$ 介于1.90 ~5.59,岩石以轻稀土元素富集和重稀土元素亏损为特征(表2和图6c)，δEu 介于0.90 ~1.11,显示正异常或弱负异常,这与花岗斑岩明显的铕负异常形成鲜明对比。从闪长岩到花岗斑岩,稀土元素总量增加,铕负异常越来越明显,轻重稀土元素分馏程度增大,表明岩浆分异程度越来越高。闪长岩富集 Rb、K、Sr 和 La 等大离子亲石元素及 Zr、Hf 等高场强元素,亏损 Ba、Ce、Ta、Nb、P 和 Ti 等元素(表2和图6d)。

5 同位素地球化学

本次选取2件花岗斑岩样品(HK1、HK3)和3件闪长岩样品(H4-186、H30-7、H30-19)进行 Sr、Nd 同位素测试,结果列于表3。

花岗斑岩 I_{Sr}介于0.706166 ~0.707025，闪长岩 I_{Sr}介于

表2 哈达庙地区中酸性侵入岩主量元素(wt%)、稀土元素及微量元素($\times10^{-6}$)分析结果

Table 2 The analyzed data of major (wt%), rare earth and trace ($\times10^{-6}$) elements of intermediate-acidic intrusive rocks from the Hadamiao area

样品号	H4-180	H30-16	H30-17	HK1	HK3	H30-4	H30-7	H30-9	H30-12	H30-14	H0-77
岩性	花岗斑岩					闪长岩					
SiO_2	74.43	74.13	77.61	74.36	75.01	57.84	59.76	54.43	55.32	60.45	55.90
TiO_2	0.21	0.27	0.07	0.25	0.29	0.69	0.61	0.56	0.54	0.66	0.67
Al_2O_3	13.62	13.32	12.40	13.66	14.09	17.26	15.82	15.79	15.61	17.47	17.49
Fe_2O_3	1.12	1.75	0.05	0.71	1.55	2.97	1.63	1.77	1.22	2.13	2.33
FeO	0.53	0.19	0.30	0.42	0.60	3.38	4.35	5.49	6.11	3.50	5.13
MnO	0.01	0.02	0.01	0.02	0.01	0.10	0.10	0.12	0.17	0.08	0.13
MgO	0.25	0.44	0.11	0.50	0.87	3.16	5.27	8.56	6.62	3.63	4.60
CaO	0.17	1.10	0.35	1.14	0.22	5.50	6.72	8.07	9.35	6.36	7.06
Na_2O	1.95	2.39	1.93	2.80	2.30	2.66	2.15	2.16	2.50	2.18	2.27
K_2O	6.25	5.63	5.51	4.99	2.92	2.68	1.27	0.36	0.64	0.41	2.02
P_2O_5	0.03	0.04	0.01	0.05	0.04	0.11	0.09	0.07	0.08	0.09	0.10
LOI	1.20	0.65	1.41	0.86	1.97	3.41	1.95	2.36	1.55	2.73	2.02
Total	99.78	99.93	99.75	99.76	99.87	99.75	99.72	99.75	99.71	99.71	99.72
K_2O/Na_2O	3.20	2.36	2.85	1.78	1.27	1.00	0.59	0.17	0.26	0.19	0.89
A/CNK	1.32	1.11	1.27	1.13	1.92	1.00	0.92	0.85	0.71	1.12	0.93
$Mg^{\#}$	22	31	36	46	44	48	62	69	62	55	53
La	37.70	31.20	18.90	37.10	28.00	17.00	10.30	4.90	4.90	7.70	14.30
Ce	71.9	62.2	30.8	76.2	48.2	34.7	20.7	11.1	10.7	16.9	28.5
Pr	7.99	6.84	3.68	8.20	5.36	4.21	2.63	1.47	1.37	2.10	3.47
Nd	27.86	24.29	12.65	28.57	18.27	16.63	11.02	6.12	6.33	8.98	14.29
Sm	4.94	4.52	2.42	4.73	3.15	3.37	2.52	1.79	1.68	2.31	3.15
Eu	0.86	0.86	0.35	0.58	0.46	1.02	0.83	0.62	0.65	0.80	0.93
Gd	4.66	4.09	2.27	4.25	2.96	3.16	2.49	1.91	1.91	2.35	3.13
Tb	0.74	0.69	0.44	0.63	0.47	0.53	0.46	0.39	0.36	0.44	0.53
Dy	4.26	3.89	2.81	3.39	2.69	3.23	2.84	2.44	2.31	2.87	3.34
Ho	0.91	0.82	0.60	0.71	0.56	0.64	0.59	0.54	0.51	0.64	0.70
Er	2.65	2.38	1.87	2.06	1.69	1.86	1.63	1.53	1.47	1.82	1.99
Tm	0.45	0.41	0.35	0.36	0.29	0.32	0.28	0.27	0.25	0.31	0.34
Yb	2.94	2.79	2.43	2.51	2.03	2.05	1.77	1.68	1.74	2.03	2.19
Lu	0.46	0.42	0.38	0.40	0.31	0.32	0.27	0.27	0.27	0.29	0.34
$\sum$REE	168.3	145.4	79.95	169.7	114.4	89.03	58.33	35.03	34.45	49.55	77.20
δEu	0.54	0.60	0.45	0.39	0.45	0.94	1.00	1.02	1.11	1.04	0.90
La/Yb	12.82	11.18	7.78	14.78	13.79	8.29	5.82	2.92	2.82	3.79	6.53
$(La/Yb)_N$	8.65	7.54	5.24	9.97	9.30	5.59	3.92	1.97	1.90	2.56	4.40
Sr	149.2	175.3	58.20	153.2	85.80	402.9	329.0	224.6	310.9	272.7	351.8
Rb	149.7	177.1	192.4	124.2	114.8	77.43	43.68	14.71	22.29	18.95	74.82
Ba	1171	842.5	408.9	1018	467.8	522.4	321.0	212.5	399.0	166.9	374.9
Th	26.90	20.10	19.10	31.40	24.60	7.70	3.50	7.20	2.70	3.00	6.90
Nb	6.93	9.79	9.45	7.71	5.81	7.19	3.21	1.91	1.99	3.21	4.68
Zr	240.9	231.7	114.2	213.2	154.6	113.0	116.1	69.14	77.26	90.90	92.15
Cs	2.80	4.60	2.80	2.30	5.30	2.60	1.70	1.40	2.10	2.10	2.70
Ga	14.99	14.01	11.17	13.03	13.62	18.23	18.03	16.07	15.39	17.15	18.82
Hf	8.19	7.59	4.46	6.74	5.26	3.34	3.24	2.03	2.39	2.61	3.48
Sc	5.80	6.70	4.00	5.80	6.70	15.60	19.70	26.10	22.90	19.10	25.90
Cr	6.40	5.30	4.20	5.90	11.70	30.80	157.3	498.3	380.5	47.60	56.60
V	19.10	25.20	11.00	35.80	43.20	117.8	143.3	168.0	150.9	137.8	171.0
Ni	6.27	7.03	1.33	4.75	6.37	22.71	60.23	132.05	96.81	20.33	22.52
Co	2.35	2.35	0.61	2.45	5.10	21.22	20.61	36.63	29.90	16.94	26.02
U	4.47	6.18	4.16	4.28	3.91	2.46	0.82	0.56	0.57	0.83	1.04
Y	26.30	22.60	17.70	21.30	16.70	18.40	16.30	14.80	14.40	17.20	19.40
Ta	0.68	0.96	1.09	0.90	0.68	0.65	0.23	0.17	0.11	0.46	0.41

注:$A/CNK = Al_2O_3/(CaO + Na_2O + K_2O)$分子数,$Mg^{\#} = 100\times[Mg^{2+}/(Mg^{2+} + Fe^{2+})]$原子数

表 3 哈达庙地区中酸性侵入岩 Sr-Nd 同位素分析结果及主要参数

Table 3 The Sr-Nd isotopic determination data and some major parameters of intermediate-acidic intrusive rocks from the Hadamiao area

样品号	Rb($\times10^{-6}$)	Sr($\times10^{-6}$)	$^{87}Rb/^{86}Sr$	$(^{87}Sr/^{86}Sr)_s$	I_{Sr}	$\varepsilon_{Sr}(t)$	Sm($\times10^{-6}$)
H4-186	90.61	635.20	0.4130	0.706372 ±9	0.704803 ±9	8.76	4.31
H30-7	43.68	329.00	0.3850	0.708149 ±6	0.706687 ±6	35.52	2.52
H30-19	56.14	285.80	0.5695	0.708915 ±9	0.706752 ±9	36.44	3.89
HK1	124.18	153.20	2.3503	0.716087 ±9	0.707025 ±9	40.39	4.73
HK3	114.80	85.80	3.8794	0.721124 ±6	0.706166 ±6	28.18	3.15
样品号	Nd($\times10^{-6}$)	$^{147}Sm/^{144}Nd$	$(^{143}Nd/^{144}Nd)_s$	$(^{143}Nd/^{144}Nd)_i$	$\varepsilon_{Nd}(t)$	t_{DM}(Ma)	$f_{Sm/Nd}$
H4-186	23.78	0.10971818	0.512539 ±5	0.512347 ±5	1.03	898	−0.44
H30-7	11.02	0.13856009	0.512502 ±6	0.512260 ±6	−0.67	1316	−0.30
H30-19	20.10	0.11710789	0.512313 ±6	0.512109 ±6	−3.62	1322	−0.40
HK1	28.57	0.10020864	0.512266 ±5	0.512088 ±5	−3.92	1189	−0.49
HK3	18.27	0.10450063	0.512327 ±5	0.512142 ±5	−2.88	1150	−0.47

注：$\varepsilon_{Nd} = [(^{143}Nd/^{144}Nd)_s/(^{143}Nd/^{144}Nd)_{CHUR} - 1] \times 10000$, $f_{Sm/Nd} = (^{147}Sm/^{144}Nd)/(^{147}Sm/^{144}Nd)_{CHUR} - 1$, $t_{DM} = 1/\lambda \times \ln\{1 + [(^{143}Nd/^{144}Nd)s - 0.51315]/[(^{147}Sm/^{144}Nd) - 0.2135]\}$, $(^{143}Nd/^{144}Nd)_{CHUR} = 0.512638$; $(^{147}Sm/^{144}Nd)_{CHUR} = 0.1967$; $(^{143}Nd/^{144}Nd)_{DM} = 0.51315$; $(^{147}Sm/^{144}Nd)_{DM} = 0.2135$

0.704803 ~ 0.706752，均低于现今大陆壳 I_{Sr} 平均值 0.719。花岗斑岩的 $\varepsilon_{Nd}(t)$ 介于 −3.92 ~ −2.88，对应的 Nd 模式年龄为 1150 ~ 1189Ma。闪长岩的 $\varepsilon_{Nd}(t)$ 介于 −3.62 ~ 1.03，略高于花岗斑岩的 $\varepsilon_{Nd}(t)$ 值，Nd 模式年龄介于 898 ~ 1322Ma，较花岗斑岩的 Nd 模式年龄稍老，较中亚造山带内花岗岩类的 Nd 模式年龄(集中在 600 ~ 800Ma，个别为 1000Ma，洪大卫等，2000；邵济安等，2002)偏老。不管是花岗斑岩还是闪长岩，$f_{Sm/Nd}$ 值均为负值，变化范围不大(−0.49 ~ −0.30)，表明源区的稀土元素 Sm、Nd 分馏不明显，Nd 模式年龄是有效的(Jahn *et al.*, 2000)。

6 讨论

6.1 岩石成因

哈达庙地区闪长岩与花岗斑岩的稀土和微量元素配分模式相似，暗示两者具有相似的岩浆源区，可能为同源岩浆不同演化阶段的产物。在微量元素蛛网图上两者均表现出富集 Rb、K 等大离子亲石元素，亏损 Nb、Ta、P、Ti 等高场强元素，显示出俯冲带岩浆岩的特征(Kelemen *et al.*, 2003)，并暗示两类岩石经历了强烈的结晶分异作用。花岗斑岩和闪长岩均富集 Zr、Hf，强烈亏损 Nb、Ta，表明其源岩可能来自地壳物质或曾遭遇地壳物质的混染，并受到与大洋板块俯冲有关的流体交代作用(La Flèche *et al.*, 1998；孙德有等，2004)。与正常的岛弧钙碱性安山岩相比(Pearce and Peate, 1995)，哈达庙地区闪长岩具有更高的 Mg#、MgO、Cr(30.80×10^{-6} ~ 498.3×10^{-6})、Ni(20.33×10^{-6} ~ 132.1×10^{-6})含量，类似于高镁安山岩(图 7)(Yogodzinski *et al.*, 1995; Tatsumi, 2001)。这种富镁闪长质岩浆的成因仍存在争议，主要观点有：(1)受交代的富集地幔部分熔融的产物(Smithies and Champion, 2000;; Zhao and Zhou, 2007)；(2)由板片熔体与地幔楔反应形成(Smithies *et al.*, 2007)；(3)由拆沉下地壳熔融的熔体与地幔橄榄岩反应形成(Gao *et al.*, 2004)；(4)消减沉积物熔融以及随后的熔体与地幔楔反应而成(Tatsumi, 2001)。无论何种成因机制，富镁闪长岩的形成均需要一个被交代的地幔源区，而差异表现为交代组分来源的不同(尹继元等，2013)。

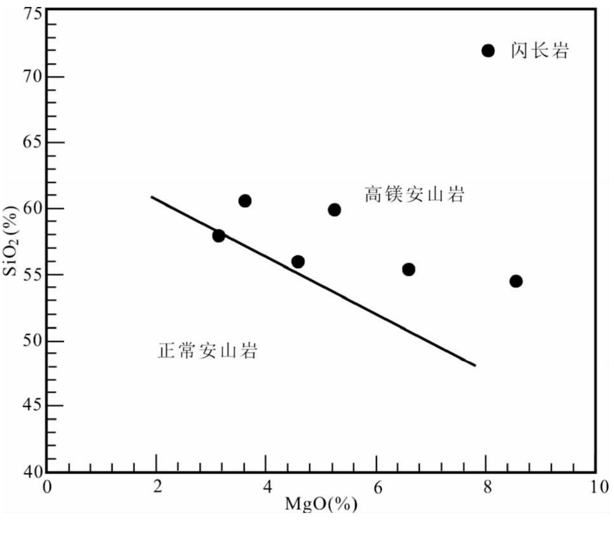

图 7 哈达庙地区闪长岩的 MgO-SiO_2 图解(底图据 McCarro and Smellie, 1998)

Fig. 7 MgO vs. SiO_2 diagram of diorite of Hadamiao area (after McCarro and Smellie, 1998)

通常认为比较高的 I_{Sr} 值是地壳来源的标志，而 $\varepsilon_{Nd}(t)$ 为负值则指示源区为地壳或富集地幔。哈达庙地区花岗斑岩和闪长岩的 $\varepsilon_{Nd}(t)$ 值介于 −3.92 ~ 1.03，I_{Sr} 值介于 0.704803

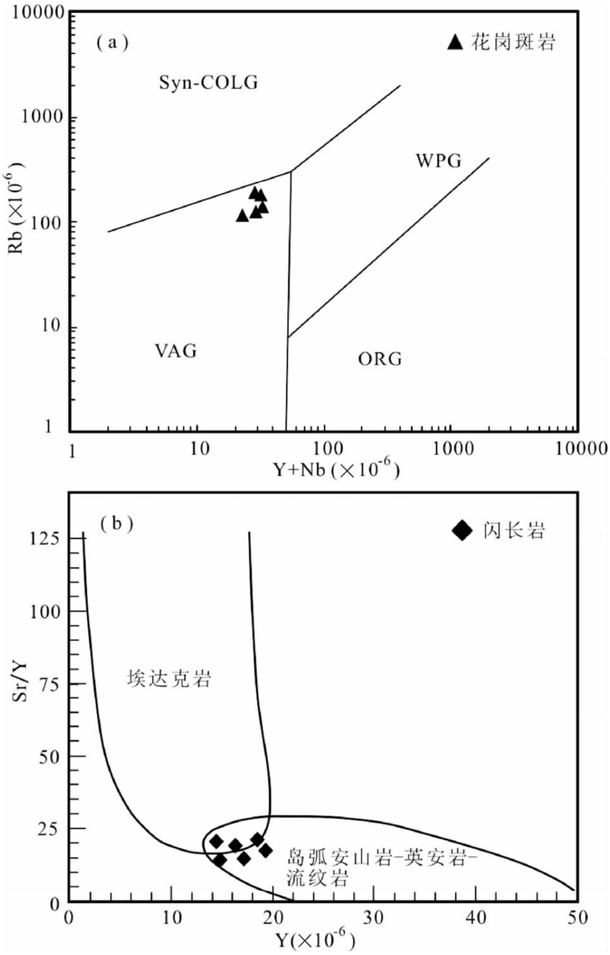

图8 哈达庙地区花岗斑岩(Y + Nb)-Rb 图解(a, 底图据 Pearce, 1996)和闪长岩 Y-Sr/Y 图解(b, 底图据 Defant and Drummond, 1993)

syn-COLG-同碰撞花岗岩;VAG-火山弧花岗岩;ORG-洋脊花岗岩;WPG-板内花岗岩

Fig. 8 (Y + Nb) vs. Rb diagram of granite porphyry (a, after Pearce, 1996) and Y vs. Sr/Y diagram of diorite (b, after Defant and Drummond, 1993) from the Hadamiao area

syn-COLG-syn-collisional granites; VAG-volcanic arc granites; ORG-oceanic ridge granites; WPG-within plate granites

~0.707025,显示出壳幔混源和新生下地壳的特征。哈达庙地区花岗斑岩和闪长岩的 $\varepsilon_{Nd}(t)$ 值高于 Jahn *et al.* (1999)归纳出的华北克拉通古老下地壳的 $\varepsilon_{Nd}(t)$ 值(-44 ~ -32),略小于东北地区和兴蒙造山带显生宙花岗岩类的 $\varepsilon_{Nd}(t)$ 值(普遍大于 0,平均值为 +2.0,吴福元等,1997;洪大卫等,2003)。中亚造山带在晚古生代-中生代发育了大规模低 I_{Sr} 值,正 $\varepsilon_{Nd}(t)$ 以及年轻 t_{DM} 模式年龄的花岗岩,它们被认为是在成岩过程中,地幔来源的新生物质加入的结果(赵振华等,1996;周泰禧等,1996; Jahn *et al.*, 2000;洪大卫等,2003;Kovalenko *et al.*, 2004; Wang *et al.*, 2004;张东阳等,2010),而在一些具有前寒武纪基底的微陆块上显示负 $\varepsilon_{Nd}(t)$ 以及较老的 t_{DM} 模式年龄,反映了部分前寒武纪地壳物质在成岩过程中有比较明显加入(Wu *et al.*, 2000; Chen *et al.*, 2000;洪大卫等,2003;Jahn *et al.*, 2000, 2004; Kovalenko *et al.*, 2004)。因此,我们认为哈达庙地区高镁闪长岩是受俯冲板片流体交代的地幔楔部分熔融形成的熔体上升过程中受到地壳物质混染的产物,而花岗斑岩很可能是闪长质岩浆结晶分异的产物。

6.2 对晚古生代古亚洲洋俯冲作用的指示

内蒙古中部地区存在南、北两条蛇绿岩带,其间夹有锡林浩特古陆,其中北部贺根山蛇绿岩与南部索伦山-西拉木伦蛇绿岩分别代表两个洋盆体系,贺根山洋闭合早于中二叠世(徐备和陈斌,1997;Robinson *et al.*, 1999;施光海等,2003;童英等,2010),而索伦山-西拉木伦缝合带所代表残留古亚洲洋在早二叠世仍处于俯冲状态(李朋武等,2006;李锦轶等,2007;Jian *et al.*, 2010)。哈达庙地区的闪长岩和花岗斑岩均形成于中二叠世,在(Y + Nb)-Rb 图解上,花岗斑岩均位于火山弧花岗岩区域(图 8a),在 Y-Sr/Y 图解上,闪长岩则基本落入岛弧火山岩区域(图 8b)。终上所述,我们认为哈达庙地区中二叠世中酸性侵入岩形成于古亚洲洋的板块俯冲环境。

7 结论

(1)哈达庙地区花岗斑岩和闪长岩的锆石 SHRIMP U-Pb 年龄分别为 271 ±3Ma 和 267 ±3Ma,形成于中二叠世。

(2)哈达庙地区花岗斑岩具有低的 Mg#、Ni 和 Cr 值,而闪长岩显示了高 MgO、Ni、Cr 等富镁闪长岩的特征,高镁闪长岩是受俯冲板片流体交代的地幔楔部分熔融形成的熔体上升过程中受到地壳物质混染的产物,而花岗斑岩为闪长质岩浆结晶分异的产物。在中二叠世,古亚洲洋在哈达庙地区发生过板块俯冲事件。

致谢 野外工作得到了中国科学院地质与地球物理研究所张宝林研究员的支持;锆石 SHRIMP U-Pb 定年工作得到了北京离子探针中心石玉若博士、颉颃强博士的帮助;Sr、Nd 同位素分析中,北京大学李文博副教授给予了帮助;中国科学院地质与地球物理研究所朱明田博士参与了野外工作和室内部分测试工作,有色金属矿产地质调查中心解洪晶博士参与了室内部分测试工作;在此一并致以诚挚的感谢。

References

Badarch G, Cunningham WD and Windley BF. 2002. A new terrane subdivision for Mongolia: Implications for the Phanerozoic crustal growth of Central Asia. Journal of Asian Earth Sciences, 21(1): 87 -110

Boynton WV. 1984. Cosmochemistry of the rare earth elements: Meteorite studies. Dev. Geochem., 2: 63 – 114

Cao CZ, Yang FL, Tian CL and Yuan Y. 1986. The ophiolite in Hegenshan district, Nei Mongol and the position of suture line between Sino-Korean and Siberian plates. In: Tang KD (ed.). Contributions to the Project of Plate Tectonics in Northern China, No. 1. Beijing: Geological Publishing House, 64 – 86 (in Chinese with English abstract)

Chen B, Jahn BW, Wilde S and Xu B. 2000. Two contrasting Paleozoic magmatic belts in northern Inner Mongolia, China: Petrogenesis and tectonic implications. Tectonophysics, 328(1 – 2): 157 – 187

Chen YJ, Chen HY, Zaw K, Pirajno F and Zhang ZJ. 2007. Geodynamic setting and tectonic model of skarn gold deposits in China: An overview. Ore Geology Reviews, 31(1 – 4): 139 – 169

Condie KC. 2005. TTGs and adakites: Are they both slab melts. Lithos, 80(1 – 4): 33 – 44

Defant MJ and Drummond MS. 1993. Mount St Helens: Potential example of the partial melting of the subducted lithosphere in a volcanic arc. Geology, 21: 547 – 550

Drummond MS, Defant MJ and Kepezhinskas PK. 1996. Petrogenesis of slab-derived trondhjemite-tonalite-dacite/adakite magmas. Transactions of the Royal Society of Edinburgh: Earth Sciences, 87 (1 – 2): 205 – 215

Gao J, Long LL, Qian Q, Huang DZ, Su W and Klemd R. 2006. South Tianshan: A Late Paleozoic or a Triassic orogen? Acta Petrologica Sinica, 22(5): 1049 – 1061 (in Chinese with English abstract)

Gao S, Rudnick RL, Yuan HL, Liu XM, Liu YS, Xu WL, Ling WL, Ayers J, Wang XC and Wang QH. 2004. Recycling lower continental crust in the North China Craton. Nature, 432 (7019): 892 – 897

He GQ and Zhu YF. 2006. Comparative study of the geology and mineral resources in Xinjiang, China, and its adjacent regions. Geology in China, 33 (3): 451 – 460 (in Chinese with English abstract)

Hong DW, Wang SG, Xie XL and Zhang JS. 2000. Genesis of positive $\varepsilon_{\mathrm{Nd}}(t)$ granitoids in the Da Hinggan Mts.-Mongolia orogenic belt and growth continental crust. Earth Science Frontiers, 7(2): 441 – 455 (in Chinese with English abstract)

Hong DW, Wang SG, Zhang JS and Wang T. 2003. Metallogenic province derived from mantle sources: A case study of Central Asian orogenic belt. Mineral Deposits, 22(1): 41 – 55 (in Chinese with English abstract)

Jahn BM, Wu FY, Lo CH and Tsai CH. 1999. Crust-mantle interaction induced by deep subduction of the continental crust: Geochemical and Sr-Nd isotopic evidence from post-collisional mafic-ultramafic intrusions of the Northern Dabie Complex, Central China. Chemical Geology, 157: 119 – 146

Jahn BW, Wu FY and Hong DW. 2000. Important crustal growth in the Phanerozoic: Isotopic evidence of granitoids from the east-central Asia. Earth Planet. Sci., 109(1): 5 – 20

Jahn BM, Windley B, Natalin B and Dobretsov N. 2004. Phanerozoic continental growth in Central Asia. Journal of Asian Earth Sciences, 23(5): 599 – 603

Jian P, Liu DY and Sun XM. 2003. SHRIMP dating of Carboniferrous Jinshajiang ophiolite in western Yunnan and Sichuan: Geochronological constraints on the evolution of the Paleo-Tethys oceanic crust. Acta Geologica Sinica, 77 (3): 317 – 327 (in Chinese with English abstract)

Jian P, Liu DY, Kröner A, Windley BF, Shi YR, Zhang W, Miao LC, Zhang LQ, Tomurhuu D. 2010. Evolution of a Permian intraoceanic arc-trench system in the Solonker suture, Central Asian Orogenic Belt, China and Mongolia. Lithos, 118(1 – 2): 169 – 190

Kelemen PB, Hanghøj K and Greene AR. 2003. One view of the geochemistry of subduction-related magmatic arcs, with an emphasis on primitive andesite and lower crust. Treatise on Geochemistry, 3: 593 – 659

Kovalenko VL, Yarmolyuk VV, Kovach VP, Kotov AB, Kozakov IK, Salnikova EB and Larin AM. 2004. Isotope provinces, mechanisms of generation and sources of the continental crust in the Central Asian mobile belt: Geological and isotopic evidence. Journal of Asian Earth Sciences, 23(5): 605 – 627

La Flèche MR, Camiré G and Jenner GA. 1998. Geochemistry of post-Acadian, Carboniferous continental intraplate basalts from the Maritimes Basin, Magdalen Islands, Québec, Canada. Chemical Geology, 148(3 – 4): 115 – 136

Li JY. 2006. Permian geodynamic setting of Northeast China and adjacent regions: Closure of the Paleo-Asian Ocean and subduction of the Paleo-Pacific plate. Journal of Asian Earth Sciences, 26(3 – 4): 207 – 224

Li JY, He GQ, Xu X, Li HQ, Sun GH, Yang TN, Gao LM and Zhu ZX. 2006. Crustal tectonic framework of northern Xinjiang and adjacent regions and its formation. Acta Geologica Sinica, 80(1): 148 – 168 (in Chinese with English abstract)

Li JY, Gao LM, Sun GH, Li YP and Wang YB. 2007. Shuangjingzi middle Triassic syn-collisional crust-derived granite in the east Inner Mongolia and its constraint on the timing of collision between Siberian and Sino-Korean paleo-plates. Acta Petrologica Sinica, 23 (3): 565 – 582 (in Chinese with English abstract)

Li JY, Qu JF, Zhang J, Liu JF, Xu WL, Zhang SH, Guo RQ, Zhu ZX, Li YP, Li YF, Wang T, Xu XY, Li ZP, Liu YQ, Sun LX, Jian P, Zhang Y, Wang LJ, Peng SH, Feng QW, Wang Y, Wang HB and Zhao XX. 2013. New developments on the reconstruction of Phanerozoic geological history and research of metallogenic geological setting of the northern China orogenic region. Geological Bulletin of China, 32(2): 207 – 219 (in Chinese with English abstract)

Li PW, Gao R, Guan Y and Li QS. 2006. Palaeomagnetic constraints on the final closure time of Solonker Linxi Suture. Journal of Jilin University (Earth Science Edition), 36(5): 744 – 758 (in Chinese with English abstract)

Liu DY, Jian P, Zhang Q, Zhang FQ, Shi YR, Shi GH, Zhang LQ and Tao H. 2003. SHRIMP dating of adakites in the Tulingkai ophiolite, Inner Mongolia: Evidence for the Early Paleozoic subduction. Acta Geologica Sinica, 77 (3): 317 – 327 (in Chinese with English abstract)

Liu J, Wu G, Zhong W and Zhu MT. 2010. Fluid inclusion study of the Duobaoshan porphyry Cu (Mo) deposit, Heilongjiang Province, China. Acta Petrologica Sinica, 26 (5): 1450 – 1464 (in Chinese with English abstract)

Liu J, Wu G, Li Y, Zhu MT and Zhong W. 2012. Re-Os sulfide (chalcopyrite, pyrite and molybdenite) systematics and fluid inclusion study of the Duobaoshan porphyry Cu (Mo) deposit, Heilongjiang Province, China. Journal of Asian Earth Sciences, 49: 300 – 312

Liu J, Mao JW, Wu G, Luo DF, Wang F, Zhou ZH and Hu YQ. 2013a. Zircon U-Pb dating for the magmatic rocks in the Chalukou porphyry Mo deposit in the northern Great Xing'an Range, China, and its geological significance. Acta Geologica Sinica, 87(2): 208 – 226 (in Chinese with English abstract)

Liu J, Wu G, Wang F, Luo DF, Hu YQ and Li TG. 2013b. Fluid inclusions and stable isotope characteristics of the Chalukou porphyry Mo deposit in Heilongjiang Province. Geology in China, 40(4): 1231 – 1251 (in Chinese with English abstract)

Liu J, Wu G, Qiu HN, Gao DZ and Yang XS. 2013c. $^{40}Ar/^{39}Ar$ dating of gold-bearing quartz vein from the Shabaosi gold deposit at the northern end of the Great Xing'an Range and its tectonic significance. Acta Geologica Sinica, 87(10): 1 – 11 (in Chinese with English abstract)

Lu YH, Li WB and Lai Y. 2009. Time and tectonic setting of hosting porphyry of the Hadamiao gold deposit in Xianghuangqi, Inner Mongolia. Acta Petrologica Sinica, 25 (10): 2615 – 2620 (in Chinese with English abstract)

Mao JW, Yang JM, Han CM and Wang ZL. 2002a. Metallogenic systems of polymetallic copper and gold deposits and related metallogenic geodynamic model in eastern Tianshan, Xinjiang. Earth Science, 27 (4): 413 – 424 (in Chinese with English abstract)

Mao JW, Yang JM, Qu WJ, Du AD, Han CM and Wang ZL. 2002b. Re-Os dating of Cu-Ni sulfide ores from Huangshandong deposit in Xinjiang and its geodynamic significance. Mineral Deposit, 21(4):

323 – 330 (in Chinese with English abstract)
Mao JW, Han CM, Wang YT, Yang JM and Wang ZL. 2002c. Geological characteristics, metallogenic model and criteria for exploration of the large south Tianshan gold metallogenic belt in Central Asia. Geological Bulletin of China, 21(12): 858 – 868(in Chinese with English abstract)
Mao JW, Xie GQ, Zhang ZH, Li XF, Wang YT, Zhang CQ and Li YF. 2005. Mesozoic large-scale metallogenic pulses in North China and corresponding geodynamic setting. Acta Petrologica Sinica, 21(1): 169 – 188 (in Chinese with English abstract)
Mao JW, Zhou ZH, Wu G, Jiang SH, Liu CL, Li HM, Ouyang HG and Liu J. 2013. Metallogenic regularity and minerogenetic series of ore deposits in Inner Mongolia and adjacent areas. Mineral Deposits, 32(4): 715 – 729(in Chinese with English abstract)
Martin H, Smithies RH, Rapp R, Moyen JF and Champion D. 2005. An overview of adakite, tonalite-trondhjemite-granodiorite (TTG), and sanukitoid: Relationships and some implications for crustal evolution. Lithos, 79(1 – 2): 1 – 24
McCarro JJ and Smellie JL. 1998. Tectonic implication of fore-arc magnesian and generation of high-magnesian andesites: Alexander island, Antarctica. Journal of the Geological Society, 155(2): 269 – 280
Nie FJ and Zhang HT. 1989. Main characteristics of the Hadamiao gold-bearing intrusive complex and its origin in the Xianghuang Banner, Nei Monggol. Geological Review, 35(4): 297 – 306(in Chinese with English abstract)
Nie FJ, Zhang HT, Sun H and Fan JT. 1989. Geological features and origin of the Hadamiao gold deposit in Inner Mongolia. Mineral Deposits, 6(2): 51 – 60(in Chinese with English abstract)
Pearce JA, Harris NBW and Tindle AG. 1984. Trace element discrimination diagrams for the tectonic interpretation of granitic rocks. J. Petrol., 25(4): 956 – 983
Pearce JA and Peate DW. 1995. Tectonic implications of the composition of volcanic arc magmas. Annual Review of Earth and Planetary Science Annual Review, 23(1): 251 – 285
Pearce JA. 1996. Source and settings of granitic rocks. Episodes, 19: 120 – 125
Peccerillo A and Taylor SR. 1976. Geochemistry of Eocene calc-alkaline volcanic rocks from the Kastamonu area, northern Turkey. Contrib. Mineral. Petrol., 58(1): 63 – 81
Robinson PT, Zhou MF, Hua XF, Reynolds P, Bai WJ and Yang JS. 1999. Geochemical constraints on the origin of the Hegenshan Ophiolite, Inner Mongolia, China. Journal of Asian Earth Sciences, 17(4): 423 – 442
Şengör AMC, Natalin BA and Burtman VS. 1993. Evolution of the Altaid tectonic collage and Paleozoic crustal growth in Eurasia. Nature, 364(6435): 209 – 307
Shao JA, Hong DW and Zhang LQ. 2002. Genesis of Sr-Nd isotopic characteristics of igneous rocks in Inner Mongolia. Geological Bulletin of China, 21(12): 817 – 822(in Chinese with English abstract)
Sheppard S, Griffin TJ, Tyler IM and Page RW. 2001. High- and low-K granites and adakites at a Palaeoproterozoic plate boundary in northwestern Australia. Journal of the Geological Society, London, 158(3): 547 – 560
Shi GH, Liu DY, Zhang FQ, Jian P, Miao LC, Shi YR, Liu DY and Tao H. 2003. Zircon SHRIMP U-Pb geochronology and significance of the Xilinhot metamorphic complex, Inner Mongolia, China. Chinese Science Bulletin, 48(20): 2187 – 2192 (in Chinese)
Smithies RH. 2000. The Archaean tonalite-trondhjemite-granodiorite (TTG) series is not an analogue of Cenozoic adakite. Earth and Planetary Science Letters, 182(1): 115 – 125
Smithies RH and Champion DC. 2000. The Archaean high-Mg diorite suite: Links to tonalite-trondhjemite-granodiorite magmatism and implications for Early Archaean crustal growth. Journal of Petrology, 41(12): 1653 – 1671
Smithies RH, Van-Kranendonk MJ and Champion DC. 2007. The Mesoarchean emergence of modern-style subduction. Gondwana Research, 11(1 – 2): 50 – 68
Streckeisen AL. 1976. Classification of the common igneous rocks by means of their chemical composition: A provisional attempt. Neues Jahrbuch fur Mineralogie, Monatshefte, 1: 1 – 15
Sun DY, Wu FY, Zhang YB and Gao S. 2004. The final closing time of the west Lamulun River-Changchun-Yanji plate suture zone: Evidence from the Dayushan granitic pluton, Jilin Province. Journal of Jilin University, 34(2): 174 – 181(in Chinese with English abstract)
Tatsumi Y. 2001. Geochemical modeling of partial melting of subducting sediments and subsequent melt-mantle interaction: Generation of high-Mg andesites in the Setouehi volcanic belt, Southwest Japan. Geology, 29: 323 – 326
Taylor SR and McLennan SM. 1985. The Continental Crust: Its Composition and Evolution. Oxford: Blackwell Scientific Publications, 54 – 374
Tong Y, Hong DW, Wang T, Shi XJ, Zhang JJ and Ceng T. 2010. Spatial and temporal distribution of granitoids in the middle segment of the Sino-Mongolian border and its tectonic and metallogenic implications. Acta Geoscientica Sinica, 31(3): 395 – 412(in Chinese with English abstract)
Wang Q and Liu XY. 1986. Paleoplate tectonics between Cathasia and Angaraland in Inner Mongolia of China. Tectonics, 5(7): 1073 – 1088
Wang T, Zheng YD, Li TB and Gao YJ. 2004. Mesozoic granitic magmatism in extensional tectonics near the Mongolian border in China and its implications for crustal growth. Journal of Asian Earth Sciences, 23(5): 715 – 729
Williams IS. 1998. U-Th-Pb Geochronology by ion microprobe. In: Mckibben MA, Shanks WC Ⅲ and Ridley WI (eds.). Applications of Microanalytical Techniques to Understanding Mineralizing Processes. Review in Economic Geology, 7: 1 – 35
Wu FY, Jahn BM and Lin Q. 1998. Isotopic characteristics of the post-orogenic granites in orogenic belt of northern China and their implications in crustal growth. Chinese Science Bulletin, 43(5): 420 – 424
Wu FY, Jahn BW, Wilde SA and Sun DY. 2000. Phanerozoic crustal growth: U-Pb and Sr-Nd isotopic evidence from the granites in northeastern China. Tectonophysics, 328(1 – 2): 89 – 113
Wu FY, Sun DY, Li HM, Jahm BM and Wilde S. 2002. A-type granites in northeastern China: Age and geochemical constraints on their petrogenesis. Chemical Geology, 187(1 – 2): 143 – 173
Xiao WJ, Windley BF, Hao J and Zhai MG. 2003. Accretion leading to collision and the Permian Solonker suture, Inner Mongolia, China: Termination of the central Asian orogenic belt. Tectonics, 22(6), 1069
Xiao WJ, Han CM, Yuan C, Sun M, Lin SF, Chen HL, Li ZL, Li JL and Sun S. 2008. Middle Cambrian to Permian subduction-related accretionary orogenesis of Northern Xinjiang, NW China: Implications for the tectonic evolution of central Asia. Journal of Asian Earth Sciences, 32(2 – 4): 102 – 117
Xu B and Chen B. 1997. The structure and evolution of a Middle Paleozoic orogenic belt between the North China and Siberian blocks, northern Inner Mongolia, China. Science in China (Series D), 27(3): 227 – 232 (in Chinese)
Yang FQ, Mao JW, Wang YT and Bierlein PF. 2006. Geology and geochemistry of the Bulong quartz-barite vein-type gold deposit in Xinjiang Uygur Autonomous Region, China. Ore Geology Reviews, 29(1): 52 – 76
Yang FQ, Mao JW, Wang YT, Zhao CS, Zhang Y and Liu YL. 2007. Major types, characteristics and metallogeneses of gold deposits in southwest Tianshan Mountains, Xinjiang. Mineral Deposits, 26(4): 361 – 379(in Chinese with English abstract)
Yang FQ, Mao JW, Bierlein PF, Pirajno F, Xia HD, Zhao CS, Ye HS and Liu F. 2009. A review of the geological characteristics and geodynamic mechanisms of Late Paleozoic epithermal gold deposits in North Xinjiang, China. Ore Geology Review, 35(2): 217 – 234
Yin JY, Chen W, Yu S, Long XP, Yuan C, Zhang Y, Li J, Sun JB and

Liu XY. 2013. Age, geochemical features and Cu-Au mineralization significance of the magnesian dioritic dykes in Baogutu area of West Junggar. Geology in China, 40(4): 1030 – 1043(in Chinese with English abstract)

Yogodzinski GM, Kay RW, Volynets ON, Koloskov AV and Kay SM. 1995. Magnesian andesite in the western Aleutian Komandorsky region: Implications for slab melting and processes in the mantle wedge. Geological Society of America Bulletin, 107(5): 505 – 519

Zhang DY, Zhang ZC, Xue CJ and Ai L. 2010. Petrology and geochemistry of the ore-forming porphyries in the Lamasu copper deposit, western Tianshan: Implications for petrogenesis. Acta Petrologica Sinica, 26(3): 680 – 694 (in Chinese with English abstract)

Zhang ZH, Mao JW, Du AD, Pirajno F, Wang ZL, Yang JM, Chai FM and Zhang ZC. 2008. Re-Os dating of two Cu-Ni sulfide deposits in northern Xinjiang and its geological significance. Journal of Asian Earth Sciences, 32(2 – 4): 204 – 217

Zhang ZH, Mao JW, Wang ZL, Pirajno F and Wang YB. 2010. Geochemical and SHRIMP U-Pb age constraints on the origin of the Qingbulake mafic-ultramafic complex in the West Tianshan Mountains, Xinjiang, Northwest China. Australian Journal of Earth Sciences, 57(6): 819 – 837

Zhang ZH, Hong W, Jiang ZS, Duan SG, Wang ZH, Li FM, Shi FP, Zhao J and Zheng RQ. 2012. Geological features, mineralization types and metallogenic setting of Late Paleozoic iron deposits in western Tianshan Mountains of Xinjiang. Mineral Deposits, 31(5): 941 – 964 (in Chinese with English abstract)

Zhou JH and Zhou MF. 2007. Geochemistry of Neoproterozoic mafic intrusions in the Panzhihua district (Sichuan Province, SW China): Implications for subduction-related metasomatism in the upper mantle. Precambrian Research, 152(1 – 2): 27 – 47

Zhao ZH, Wang ZG, Zou TR and Masuda A. 1996. Study on petrogenesis of alkali-rick intrusive rocks of Ulungur, Xinjiang. Geochimica, 25(3): 205 – 220 (in Chinese with English abstract)

Zhou TX, Chen JF and Li XM. 1996. Origin of high $\varepsilon_{Nd}(t)$ granites from Alatao Mountain, Xinjiang. Scientia Geologica Sinica, 31(1): 71 – 79 (in Chinese with English abstract)

Zhou ZH, Lü LS, Feng JR, Li C and Li T. 2010. Molybdenite Re-Os ages of Huanggang skarn Sn-Fe deposit and their geological significance, Inner Mongolia. Acta Petrologica Sinica, 26(3): 667 – 679(in Chinese with English abstract)

Zhou ZH, Mao JW and Lyckberg P. 2012. Geochronology and isotopic geochemistry of the A-type granites from the Huanggang Sn-Fe deposit, southern Great Hinggan Range, NE China: Implication for their origin and tectonic setting. Journal of Asian Earth Sciences, 49: 272 – 286

附中文参考文献

曹从周，杨芳林，田昌烈，袁朝. 1986. 内蒙古贺根山地区蛇绿岩及中朝板块和西伯利亚板块之间的缝合带位置. 见：唐克东编. 中国北方板块构造论文集. 北京：地质出版社，64 – 86

高俊，龙灵利，钱青，黄德志，苏文，Klemd R. 2006. 南天山：晚古生代还是三叠纪碰撞造山带？岩石学报，22(5)：1049 – 1061

何国琦，朱永峰. 2006. 中国新疆及其邻区地质矿产对比研究. 中国地质，33(3)：451 – 460

洪大卫，王式洸，谢锡林，张季生. 2000. 兴蒙造山带正 $\varepsilon_{Nd}(t)$ 值花岗岩的成因和大陆地壳生长. 地学前缘，7(2)：441 – 455

洪大卫，王式洸，谢锡林，张季生，王涛. 2003. 试析地幔来源物质成矿域-以中亚造山带为例. 矿床地质，22(1)：41 – 55

简平，刘敦一，孙晓猛. 2003. 滇川西部金沙江石炭纪蛇绿岩 SHRIMP 测年：古特提斯洋壳盆演化的同位素年代学制约. 地质学报，77(2)：217 – 228

李锦轶，何国琦，徐新，李华芹，孙桂华，杨天南，高立明，朱志新. 2006. 新疆北部及邻区地壳构造格架及其形成过程的初步探讨. 地质学报，80(1)：148 – 168

李锦轶，高立明，孙桂华，李亚萍，王彦斌. 2007. 内蒙古东部双井子中三叠世同碰撞壳源花岗岩的确定及其对西伯利亚与中朝古板块碰撞时限的约束. 岩石学报，23(3)：565 – 582

李锦轶，曲军锋，张进，刘建峰，徐文良，张拴宏，郭瑞清，朱志新，李亚萍，李永飞，王涛，徐学义，李智佩，柳永清，孙立新，简平，张昱，王励嘉，彭树华，冯乾文，王煜，王洪波，赵西西. 2013. 中国北方造山区显生宙地质历史重建与成矿地质背景研究进展. 地质通报，32(2)：207 – 219

李朋武，高锐，管烨，李秋生. 2006. 内蒙古中部索伦林西缝合带封闭时代的古地磁分析. 吉林大学学报(地球科学版)，36(5)：744 – 758

刘敦一，简平，张旗，张福勤，石玉若，施光海，张履桥，陶华. 2003. 内蒙古图林凯蛇绿岩中埃达克岩 SHRIMP 测年：早古生代洋壳消减的证据. 地质学报，77(3)：317 – 327

刘军，武广，钟伟，朱明田. 2010. 黑龙江省多宝山斑岩型铜(钼)矿床成矿流体特征及演化. 岩石学报，26(5)：1450 – 1464

刘军，毛景文，武广，罗大峰，王峰，周振华，胡妍青. 2013a. 大兴安岭北部岔路口斑岩钼矿床岩浆岩锆石 U-Pb 年龄及其地质意义. 地质学报，87(2)：208 – 226

刘军，武广，王峰，罗大锋，胡妍青，李铁刚. 2013b. 黑龙江省岔路口斑岩钼矿床流体包裹体和稳定同位素特征. 中国地质，40(4)：1231 – 1251

刘军，武广，邱华宁，高德柱，杨鑫生. 2013c. 大兴安岭北部砂宝斯金矿床含金石英脉 $^{40}Ar/^{39}Ar$ 年龄及其构造意义. 地质学报，87(10)：1 – 11

鲁颖淮，李文博，赖勇. 2009. 内蒙古镶黄旗哈达庙金矿床含矿斑岩体形成时代和成矿构造背景. 岩石学报，25(10)：2615 – 2620

毛景文，杨建民，韩春明，王志良. 2002a. 新疆东天山铜金矿床成矿系统和成矿地球动力学过程. 地球科学，27(4)：413 – 424

毛景文，杨建民，屈文俊，杜安道，韩春明，王志良. 2002b. 新疆黄山东铜镍硫化物矿床 Re-Os 同位素测定及其地球动力学意义. 矿床地质，21(4)：323 – 330

毛景文，韩春明，王义天，杨建民，王志良. 2002c. 中亚地区南天山大型金矿带的地质特征、成矿模型和勘查准则. 地质通报，21(12)：858 – 868

毛景文，谢桂青，张作衡，李晓峰，王义天，张长青，李永峰. 2005. 中国北方中生代大规模成矿作用的期次及其地球动力学背景. 岩石学报，21(1)：169 – 188

毛景文，周振华，武广，江思宏，刘成林，李厚民，欧阳荷根，刘军. 2013. 内蒙古及邻区矿床成矿规律与成矿系列. 矿床地质，32(4)：715 – 729

聂凤军，张洪涛. 1989. 内蒙古哈达庙含金侵入杂岩体的基本地质特征及岩体成因问题. 地质论评，35(4)：297 – 306

聂凤军，张洪涛，孙浩，樊建廷. 1989. 内蒙古哈达庙金矿床地质特征及矿床成因探讨. 矿床地质，6(2)：51 – 60

邵济安，洪大卫，张履桥. 2002. 内蒙古火成岩 Sr-Nd 同位素特征及成因. 地质通报，21(12)：817 – 822

施光海，刘敦一，张福勤，简平，苗来成，石玉若，陶华. 2003. 中国

内蒙古锡林郭勒杂岩 SHRIMP 锆石 U-Pb 年代学及意义. 科学通报, 48(20): 2187 - 2192

孙德有, 吴福元, 张艳斌, 高山. 2004. 西拉木伦-长春-延吉板块缝合带的最后闭合时间——来自吉林大玉山花岗岩体的证据. 吉林大学学报, 34(2): 174 - 181

童英, 洪大卫, 王涛, 史兴俊, 张建军, 曾涛. 2010. 中蒙边境中段花岗岩时空分布特征及构造和找矿意义. 地球学报, 31(3): 395 - 412

吴福元, 江博明, 林强. 1997. 中国北方造山带造山后花岗岩的同位素特点与地壳生长意义. 科学通报, 42(20): 2188 - 2192

徐备, 陈斌. 1997. 内蒙古北部华北板块与西伯利亚板块之间中古生代造山带的结构及演化. 中国科学(D 辑), 27(3): 227 - 232

杨富全, 毛景文, 王义天, 赵财胜, 张岩, 刘亚玲. 2007. 新疆西南天山金矿床主要类型、特征及成矿作用. 矿床地质, 26(4): 361 - 379

尹继元, 陈文, 喻顺, 龙晓平, 袁超, 张彦, 李洁, 孙敬博, 刘新宇. 2013. 西准噶尔包古图富镁闪长质岩墙的时代、地球化学特征以及铜金成矿意义. 中国地质, 40(4): 1030 - 1043

张东阳, 张招崇, 薛春纪, 艾羽. 2010. 西天山喇嘛苏铜矿成矿斑岩的岩石学、地球化学特征及成因探讨. 岩石学报, 26(3): 680 - 694

张作衡, 洪为, 蒋宗胜, 段士刚, 王志华, 李凤鸣, 石福品, 赵军, 郑仁乔. 2012. 新疆西天山晚古生代铁矿床的地质特征、矿化类型及形成环境. 矿床地质, 31(5): 941 - 964

赵振华, 王中刚, 邹天人, 增田彰正. 1996. 新疆乌伦古富碱侵入岩成因探讨. 地球化学, 25(3): 205 - 220

周泰禧, 陈江峰, 李学明. 1996. 新疆阿拉套山花岗岩类高 ε_{Nd} 值的成因探讨. 地球科学, 31(1): 71 - 79

周振华, 吕林素, 冯佳睿, 李超, 李涛. 2010. 内蒙古黄岗矽卡岩型锡铁矿床辉钼矿 Re-Os 年龄及其地质意义. 岩石学报, 26(3): 667 - 679